

A HIGH-ORDER VISCOELASTIC FRACTIONAL ELEMENT APPLIED TO MODELING OVINE ARTERIAL WALL BEHAVIOR

Jorge M. Pérez Zerpa¹, Alfredo Canelas¹, Berardi Sensale¹, Daniel Bia
Santana², Ricardo L. Armentano³

¹ Instituto de Estructuras y Transporte (IET)
Facultad de Ingeniería, Universidad de la República.
Julio Herrera y Reissig 565, Montevideo, Uruguay, PC 11300
e-mail: jperez@fing.edu.uy, web page: <http://www.fing.edu.uy/iet>

² Departamento de Fisiología, CUiiDARTE
Facultad de Medicina, Universidad de la República
General Flores 2125, Montevideo, Uruguay, PC 11800

³ Grupo de Ingeniería Aplicada a los Procesos Biológicos y Agrícolas
Centro Universitario Regional Noroeste, Universidad de la República
Florida 1051, Paysandú, Uruguay

Key words: Viscoelasticity, Fractional Calculus, Arterial Wall Mechanics.

Abstract. Viscoelastic models have been widely used for modeling and understanding the behavior of materials, however, real materials are not describable by models with a small number of springs and dashpots. In order to improve the ability of these models, in the twentieth century it was introduced the spring-pot element. The models that include a spring-pot are called Fractional Viscoelastic Models (FVMs) and have provided promising results for modeling materials such as polymers and living tissue. Our aim is to improve the accuracy of these models through the use of a modified version of the spring-pot, called high-order spring-pot (HOSP).

In this article we implement a numerical method for characterization of mechanical properties of FVMs from stress strain measures. We validate the implementation using artificially generated data with and without noise added. Afterwards, we apply the method to ovine arterial wall data presented in the literature. The method is applied using the spring-pot and the HOSP.

The results obtained using the artificial data, show that the method is able to characterize the mechanical parameters even in presence of low-level noise. For the experimental data the results show a notable improvement using the HOSP. We conclude that the FMVs are improved when a high-order spring-pot is included. In particular, it was shown that these models are appropriate for modeling arterial wall behavior, which represent better results in computational simulations of the arterial wall mechanics.

1 Introduction

The behavior of viscoelastic materials is usually represented by simple models composed by elastic and viscous elements, which usually are linear springs and dashpots respectively. As presented in [1], living tissues have a viscoelastic behavior, in the literature we can find applications of these models to a wide range of different tissues [2, 3, 4]. However, there exists a particular interest in the modeling of the arterial wall behavior, motivated by the importance of the Atherosclerotic Cardiovascular Disease in the death toll [5]. As it is stated by Lakes in [6], the models formed by a small number of springs and dashpots are used with a pedagogic role and real materials are not usually describable by these models, thus more complex models are required.

Fractional viscoelastic models (FVMs) are those viscoelastic models that include at least one fractional element, also known as spring-pot. The spring-pot element represents an intermediate behavior between a linear spring and a linear dashpot. This intermediate behavior is mathematically represented by a fractional derivative, thus the stress is proportional to the fractional derivative of the strain, i.e. $\sigma \propto D^\alpha \varepsilon$, where the derivative order α is considered another mechanical parameter, called fractional parameter. In the FVMs presented in the literature the fractional parameter is considered within the interval $[0, 1]$.

FVMs have proven to be well suited for modeling the behavior of real complex materials such as anisotropic structural elements [7], polymers [8] and living tissue. For living tissues, the FVMs have been presented as a good alternative for the modeling of arterial wall mechanics [9, 10].

In [11] are presented positive results for the use of higher order models, where the constitutive relations derivative orders are higher than 1. This high-order behavior is obtained by introducing several spring-pot elements in series and parallel in rheological models. In this paper we use a fractional element that we call high-order-spring-pot (HOSP), which is defined by letting the upper bound of α to be 2. We use FVMs with one HOSP and prove its ability to reproduce the behavior of arterial wall with higher accuracy. A thermodynamic justification of the upper bound assumed for the fractional parameter can be shown through a procedure similar to the one presented in [12].

In this Section 2 we will present the basic concepts of fractional calculus, some important properties for the Fourier transform use and finally present the three viscoelastic models used through the article.

In Section 3 we describe a method for characterization of mechanical parameters of FVMs, including the fractional parameter α . The numerical method obtains the parameters through the solution of an inverse problem, using a fitness function given by the Fourier coefficients of the signals.

A validation is performed by obtaining numerical results which are presented in Section 4. The experimental data used is part of the data obtained at the [4] pressure and diameter of healthy ovine arterial wall. Finally conclusions are obtained about the

advantages of the use of the HOSP and possible interpretations of the results.

2 Preliminaries

2.1 Fractional calculus

The Fractional Calculus theory introduces a generalization of the derivative of a function for non integer order. There are several definitions for fractional derivatives of a function, in this paper we will consider the Riemann-Louville definition with lower terminal as $-\infty$, given by the following expression

$$D^\alpha f(t) = \frac{1}{\Gamma(n - \alpha)} \int_{-\infty}^t \frac{f^{(n)}(\tau)}{(t - \tau)^{\alpha+1-n}} d\tau \quad n - 1 < \alpha < n. \quad (1)$$

This derivative is described as a good definition for steady-state processes such as response of viscoelastic materials for a given periodic load [13]. The idea used is that the structural element whose stress response is an intermediate between a spring and a dashpot, thus a zero or first order derivative of the strain.

Let us remark the following property:

$$D^\alpha e^{i\omega t} = (i\omega)^\alpha e^{i\omega t} \quad \forall t \in \mathbb{R} \quad \forall \alpha \in \mathbb{R}. \quad (2)$$

For the numerical computing of the value i^α we use the formula $i^\alpha = \cos(\alpha \frac{\pi}{2}) + i \sin(\alpha \frac{\pi}{2})$ which is also given by the numerical calculation implemented by the numerical software GNU-Octave.

2.2 Applying the DFT

Given $y(t)$, a periodic continuous function for a magnitude y , let us consider that an acquisition is performed in N times starting at $t = 0$. The discrete signal is given by

$$y_n = y(T \cdot n) \quad n = 0, \dots, N - 1, \quad (3)$$

where T is the time between samples. If $f_s = 1/T$ is the sampling frequency (the number of samples per time unit) then, we can write $y_n = y(\frac{n}{f_s})$. Let us define the Discrete Fourier Transformation DFT: $\mathbb{C}^N \rightarrow \mathbb{C}^N$, as a vectorial function $\mathbf{Y} = \text{DFT}(\mathbf{y})$, where the k -th entry of \mathbf{Y} is given by

$$Y_k = \sum_{n=0}^{N-1} y_n \cdot e^{-i\omega_k \frac{n}{f_s}} \quad k = 0, \dots, N - 1, \quad (4)$$

where $\omega_k = 2\pi k \frac{f_s}{N}$ is the k -th frequency. The Inverse DFT is the inverse function of the DFT transform, i.e. $\mathbf{y} = \text{IDFT}(\mathbf{Y})$, and the n -th entry of \mathbf{y} is given by

$$y_n = \frac{1}{N} \sum_{k=0}^{N-1} Y_k \cdot e^{i\omega_k \frac{n}{f_s}} \quad n = 0, \dots, N - 1. \quad (5)$$

Let us assume that the continuous function y can be decomposed as a sum of exponential functions, and by using the Equation (2) we obtain

$$y(t) = \frac{1}{N} \sum_{k=0}^{N-1} Y_k e^{i\omega_k t} \quad D^\alpha y(t) = \frac{1}{N} \sum_{k=0}^{N-1} (i\omega_k)^\alpha Y_k e^{i\omega_k t}. \quad (6)$$

If we consider the times $t = n/f_s$ we can see that the coefficients of these decompositions can be obtained by using the DFT.

2.3 Fractional viscoelastic model

In this section we describe the fractional variation of the well known Standard linear solid viscoelastic model [14], called Fractional Standard Linear Solid model (FSLs). In this constitutive model the material response is represented by an arrangement of two springs and a spring-pot, as can be seen in Figure 1. The material parameters E_0 and E_1 correspond to the stiffness of the springs and η_1 and α are the viscosity and fractional parameter of the spring-pot respectively. All the constants are positive. The stress response of the fractional element is proportional to the fractional derivative of the deformation, as seen in the following equation

$$\sigma = E_1^{1-\alpha} \eta_1^\alpha D^\alpha \varepsilon \quad (7)$$

where α is the fractional parameter. In the literature this parameter is considered a real number in the domain $[0, 1]$. However it can be shown that it is thermodynamically admissible to let α be in the domain $[0, 2]$.

The model provides the following constitutive equation

$$\sigma + \tau_\sigma D^\alpha \sigma = E_0 ((\varepsilon - \varepsilon_0) + \tau_\varepsilon D^\alpha \varepsilon) \quad (8)$$

where

$$\tau_\sigma = \left(\frac{\eta_1}{E_1} \right)^\alpha, \quad \tau_\varepsilon = \frac{E_1 + E_0}{E_0} \tau_\sigma, \quad (9)$$

and ε_0 is a reference strain, or the strain corresponding to a stress-free configuration.

It is important to say that the parameters τ have dimension of $[\text{time}^\alpha]$. It is easy to see that this model represents the Standard Linear Solid model when considering $\alpha = 1$.

3 Characterization method

Let us consider the FSLs constitutive model given by five material parameters, which can be separated in a fractional parameter α and other four mechanical parameters represented by the vector \mathbf{x} . Using this notation the constitutive equation is,

$$\sigma + x_4 D^\alpha \sigma = -x_1 + x_2 \varepsilon + x_3 D^\alpha \varepsilon. \quad (10)$$

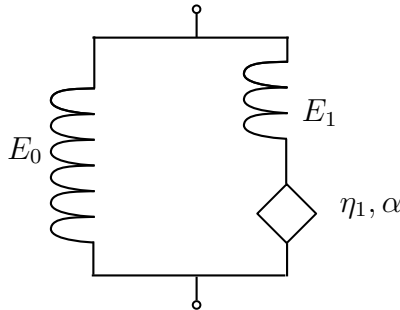


Figure 1: Fractional Standard Linear Solid model

Let us consider that stresses and strains are acquired in N times. Applying the DFT to both terms and using the properties presented in Section 2.2 we obtain the following identity:

$$(\mathbf{I} + x_4 \mathbf{\Lambda}_\alpha) \mathbf{Q} + x_1 \mathbf{D} - (x_2 \mathbf{I} + x_3 \mathbf{\Lambda}_\alpha) \mathbf{U} = 0 \quad (11)$$

where \mathbf{Q} and \mathbf{U} the DFT vectors of the signals acquired for σ and ε , respectively, $\mathbf{\Lambda}_\alpha$ is a diagonal matrix with coefficients $(\mathbf{\Lambda}_\alpha)_{nn} = (i\omega_n)^\alpha$, and \mathbf{D} is a vector with $D_i = \delta_{i1}N$. Let us consider that the strain and stress are measured and represented by the signals $\tilde{\varepsilon}$ and $\tilde{\sigma}$ respectively, and their respective DFT coefficient vectors represented with $\tilde{\mathbf{U}}$, $\tilde{\mathbf{Q}}$. We denote the strain and stress solution to (10) by ε and σ , these are the signals given by the model for certain mechanical parameters.

In a similar way as it is done in [4], we assume that either the stress or the strain given by the model is equal to the measured signal. For the numerical results presented in this paper we will assume that the stress, and therefore its DFT vector, has no error, thus $\tilde{\mathbf{Q}} = \mathbf{Q}$. We can obtain the strain DFT vector given by the model from Equation 11 obtaining:

$$U_n(\mathbf{x}, \alpha) = \frac{(1 + x_4(i\omega_n)^\alpha)\tilde{Q}_n + x_1N\delta_{n0}}{x_2 + x_3(i\omega_n)^\alpha} \quad n = 0, \dots, N - 1. \quad (12)$$

The problem of characterization thus is to determine the best parameters to fit the experimental strain with the one given by the model. Finally the characterization problem is given by

$$(C) \begin{cases} \min_{\mathbf{x}, \alpha} f(\mathbf{x}, \alpha) \\ \text{subject to} \\ x_i \geq 0 \quad i = 2, \dots, 4 \\ \mathbf{x} \in \mathbb{R}^4 \quad \alpha \in I_\alpha \end{cases} \quad \text{with} \quad f(\mathbf{x}, \alpha) = \frac{\|\mathbf{U}(\mathbf{x}, \alpha) - \tilde{\mathbf{U}}\|^2}{\|\tilde{\mathbf{U}}\|^2}, \quad (13)$$

where f is the fitness, given by the relative error of the DFT coefficients of the strain of the model, and I_α is a given real interval. This inverse problem is solved using an iterative numerical method which is presented at next.

Since the fractional parameter varies in a real interval, the problem (C) is solved for all fractional parameters in a given discrete set of values $S_\alpha = \{\alpha_s + i\Delta\alpha \mid i = 1, \dots, N_\alpha\}$.

After solving the problem (C) for all values $\alpha \in S_\alpha$ we define the optimal fractional parameter α^* the one with lower fitness f and the mechanical parameters \mathbf{x}^* are the correspondent solution of (C) for that parameter. In a schematic notation can be written as

$$\mathbf{x}^* = \arg \min_{\mathbf{x}} (\arg \min_{\alpha \in S_\alpha} f(\mathbf{x}, \alpha)). \quad (14)$$

Although the DFT gives us a vector of coefficients with as many entries as signal measurements, we will use a certain number of coefficients. associated with the first harmonics of the fundamental frequency of the signal. This reduced DFT vector is used for the fitness evaluation in Equation (13), at the characterization method implemented.

4 Results

In order to obtain results about the characterization method presented three we solve one example with artificially generated data. After that, the characterization method is applied to the experimental data. The characterization is done using the `sqp` solver of the optimization package of the GNU-Octave software.

Error measure A relative error is obtained by using the L-2 norm is used to measure the misfit after characterization. The error measures the misfit between the strain given by the model ε and the solution strain $\tilde{\varepsilon}$. The expression of the error is given by

$$Error = \frac{\|\varepsilon - \tilde{\varepsilon}\|_{L_2}}{\|\tilde{\varepsilon}\|_{L_2}} = \frac{\sqrt{\int_0^T |\varepsilon(t) - \tilde{\varepsilon}(t)|^2 dt}}{\sqrt{\int_0^T |\tilde{\varepsilon}(t)|^2 dt}}. \quad (15)$$

4.1 Example 1 - Artificial data

In this example the characterization method is applied to artificially generated data. The data is generated using the FLSL model with known mechanical parameters, and also is generated another data set by adding noise. The goal of this example is to verify that the characterization method effectively obtains the mechanical parameters used to generate data accurately even in the presence of low level noise.

Strain values are produced using the following formula

$$\tilde{\varepsilon}(t) = \varepsilon_{0c} + \sum_{i=1}^2 \varepsilon_{ic} \cos(\lambda_i t) + \varepsilon_{is} \sin(\lambda_i t) \quad (16)$$

where the frequencies are $\lambda_i = 2\pi 1.2 i$, and the amplitudes are $\varepsilon_{0c} = 0.15$, $\varepsilon_{1c} = 0.075$, $\varepsilon_{1s} = 0.025$, $\varepsilon_{2c} = 0.3\varepsilon_{1c}$, and $\varepsilon_{2s} = 0.3\varepsilon_{1s}$. The values of $\tilde{\sigma}$ are calculated using the FLSL model with the following mechanical parameters $E = 1000$ Pa, $\tau_\varepsilon = 0.1 \text{ sec}^\alpha$,

$\tau_\sigma = 0.01 \text{ sec}^\alpha$, and $\alpha = 0.64$. Also $\varepsilon_0 = 0$. The noise addition to the data is obtained as in [8] through the following expression

$$\hat{\varepsilon}(t) = \tilde{\varepsilon}(t) + v(t)\xi\sqrt{\text{var}(\tilde{\varepsilon})} \quad \hat{\sigma}(t) = \tilde{\sigma}(t) + w(t)\xi\sqrt{\text{var}(\tilde{\sigma})} \quad (17)$$

where $v(t)$ and $w(t)$ are standard distribution vectors with zero mean and unit deviation and ξ is the noise level.

The characterization method is applied for each value of α in the discrete set S_α obtained from the interval $I_\alpha = [0.2, 1]$ with a step 0.005. In Figure 2 we can see the optimum fitness obtained for each value of α for both series of data, with and without noise.

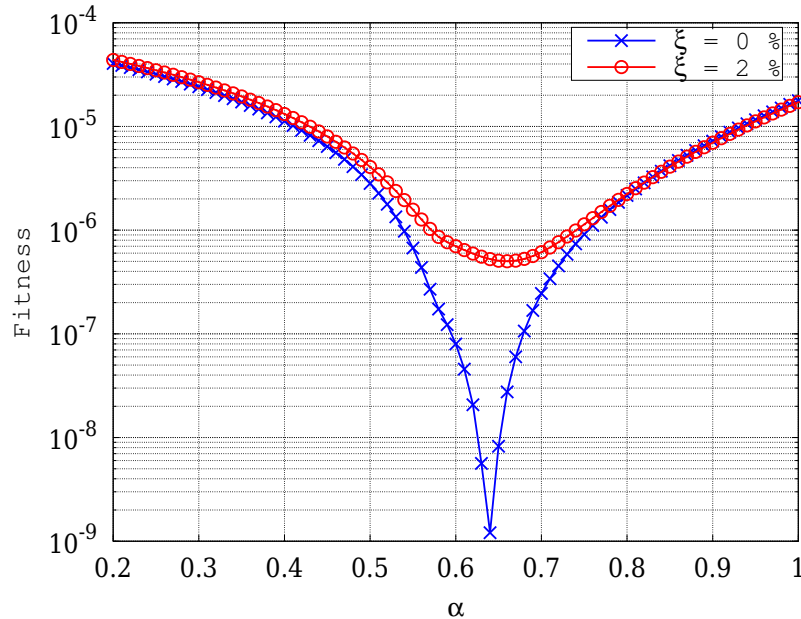


Figure 2: Optimum fitness graph of the example 1.

The numerical results obtained are presented in Table 1. The error of the fractional parameter in the data without noise is given by the precision used at the search, in this case is 0.005 which represents an error below 0.7%. It is important to remark also that the residual strain ε_0 obtained by the method can be neglected against the strain values of the signal.

In Figure 3 at left we can see the hysteresis with the deformation given by the model using the optimal mechanical parameters (crosses) and the hysteresis of the solution data (circles). At the same figure at right we can see the both hysteresis for data with noise.

Table 1: Results example 1

Variable	Solution	Data 1	Rel. Error %	Data 2	Rel. Error %
ε_0	0	$1.61 \cdot 10^{-5}$	-	$1.54 \cdot 10^{-5}$	-
E (Pa)	1000.00	1000.03	0.00	1010.66	0.00
τ_ε (sec $^\alpha$)	0.10	0.09984	0.17	0.09478	0.17
τ_σ (sec $^\alpha$)	0.01	0.00989	1.1	0.01116	11.6
α	0.64	0.64	< 0.7	0.66	3.1
fitness	-	$1.21 \cdot 10^{-9}$	-	$5.01 \cdot 10^{-7}$	-
Error	-	$2.81 \cdot 10^{-4}$	-	$76.12 \cdot 10^{-4}$	-

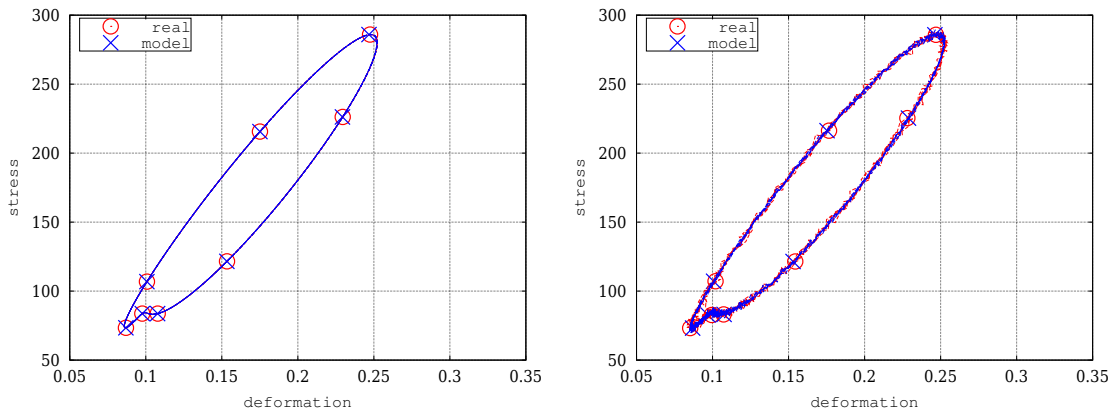


Figure 3: Example 1: Left hysteresis results for data without noise, Right results for data with noise.

4.2 Example 2 - Experimental data

The experimental data used in this example is part of the data obtained in [4], from measurements of pressure and average radius of a healthy Ascending Aorta of a Merino sheep. Considering that for the vessel studied here can be assumed $h/r \approx 0.1$, where h is the thickness and r is the average radius of the vessel, we can use a similar model to the one presented in [4] and calculate the circumferential stress and strain as thin-wall vessels

$$\sigma_{\theta\theta} = \frac{pr}{h}, \quad \varepsilon_{\theta\theta} = \frac{r - r_0}{r_0}, \tag{18}$$

where p is the internal pressure and r the average radius. The radial and axial component of the stress are neglected [1, 15]. The data was obtained with a 200 Hz sample frequency and converted to strain and strains considering the reference radius $r_0 = 9.66$ mm. Pressure is measured in millimeters of Mercury and the diameter in millimeters.

The characterization was done for $I_\alpha = [0, 1]$ and $I_\alpha = [0, 2]$, and the step for α was considered 0.001. The results are presented in Table 2.

Table 2: Results example 2

Variable	$I_\alpha = [0, 1]$	$I_\alpha = [0, 2]$
$E(\text{mmHg})$	5812.58	7785.56
ε_0	-0.053	-0.0019
τ_ε	0.0327791	0.00763564
τ_σ	0.00697166	0.00284591
α	1.0	1.644
Error (%)	5.394	2.747
Fitness	13.369 e-4	1.5255 e-4

We can see that the use of the HOSP element ($I_\alpha = [0, 2]$) reduces the Error by 50%. In Figure 4 at the left we can see the hysteresis obtained at the optimum with $I_\alpha = [0, 1]$, where the experimental data is red with circles and the model is blue with cross markers. At the right are shown the results for $I_\alpha = [0, 2]$, where it is clearly shown the improvement in the fit.

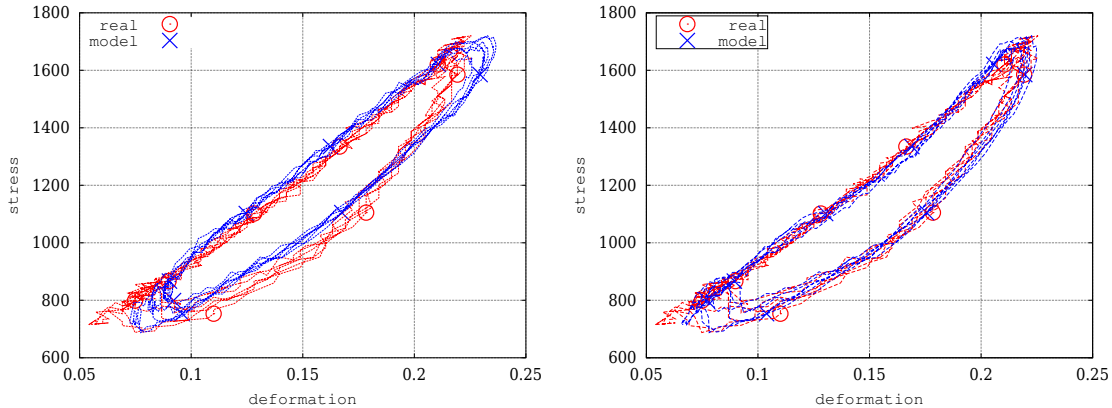


Figure 4: Example 2: left Hysteresis experimental and numerical for $I_\alpha = [0, 1]$, right results for $I_\alpha = [0, 2]$

In Figure 5 we can see the optimal fitness graph for all α in the interval $[0, 2]$. The fitness graph obtained is similar to the one obtained in Example 1 with the data with noise.

5 Conclusions

In this paper it was presented a high-order fractional viscoelastic element called HOSP that was included in a Fractional Standard Linear Solid viscoelastic model. After that, a characterization method for mechanical parameters of FVMs was described and implemented in GNU-Octave. Looking at the results obtained for the Example 1 we can

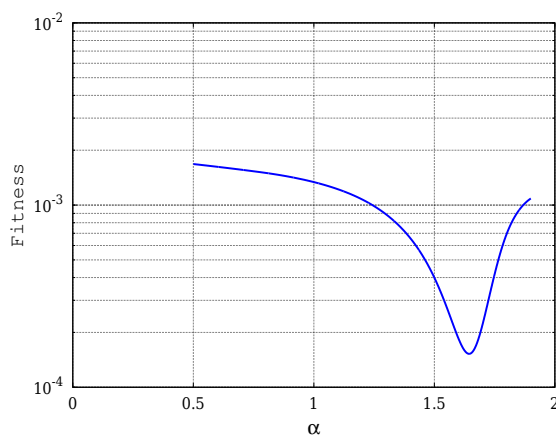


Figure 5: Example 2 Optimal fitness graph

conclude that the proposed method is adequate for characterization of the fractional parameter α even if data has a certain level of noise.

After validation, the method was applied to experimental data of an ovine arterial wall. The results obtained for $I_\alpha = [0, 1]$ are coherent with those presented in [4], thus we confirmed that the characterization method is working properly. When the interval $I_\alpha = [0, 2]$ was set, it was seen that the optimal fractional parameter is greater than one, and that the new bound considered improves significantly the accuracy of the fit of the strain.

Since in the literature the fractional parameter is bounded by one, it is a challenging task to obtain physiological interpretations for a higher fractional parameter. However, even if no interpretation is provided yet, a better modeling is obtained, which means, for instance, improvements in simulation of the arterial wall behavior.

This result enhances the importance of the fractional viscoelastic models. By using HOSPs, we can fit complex behavior in a wide range of materials, such as the arterial wall considered in this paper.

Acknowledgement

The authors would like to thank the financial support of Agencia Nacional de Investigación e Innovación (FMV-3-2011-1-6125) and Comisión Sectorial de Investigación Científica.

References

- [1] Yuan Cheng Fung. *Biomechanics, Mechanical Properties of Living Tissues*. Springer New York, New York, NY, 1981.
- [2] C Then, T J Vogl, and G Silber. Method for characterizing viscoelasticity of human

- gluteal tissue. *Journal of Biomechanics*, 45(7):1252–8, April 2012.
- [3] Man Zhang, Priya Nigwekar, Benjamin Castaneda, Kenneth Hoyt, Jean V Joseph, Anthony di Sant’Agnese, Edward M Messing, John G Strang, Deborah J Rubens, and Kevin J Parker. Quantitative characterization of viscoelastic properties of human prostate correlated with histology. *Ultrasound in medicine & biology*, 34(7):1033–42, July 2008.
- [4] Daniela Valdez-Jasso, Mansoor A. Haider, H. T. Banks, Daniel Bia Santana, Yanina Zócalo Germán, Ricardo L. Armentano, and Mette S. Olufsen. Analysis of viscoelastic wall properties in ovine arteries. *IEEE transactions on biomedical engineering*, 56(2):210–9, February 2009.
- [5] Morteza Naghavi, Peter Libby, Erling Falk, S Ward Casscells, Silvio Litovsky, John Rumberger, Juan Jose Badimon, Christodoulos Stefanadis, Pedro Moreno, Gerard Pasterkamp, Zahi Fayad, Peter H Stone, Sergio Waxman, Paolo Raggi, Mohammad Madjid, Alireza Zarrabi, Allen Burke, Chun Yuan, Peter J Fitzgerald, David S Siscovick, Chris L de Korte, Masanori Aikawa, K E Juhani Airaksinen, Gerd Assmann, Christoph R Becker, James H Chesebro, Andrew Farb, Zorina S Galis, Chris Jackson, Ik-Kyung Jang, Wolfgang Koenig, Robert a Lodder, Keith March, Jasenka Demirovic, Mohamad Navab, Silvia G Priori, Mark D Reikhter, Raymond Bahr, Scott M Grundy, Roxana Mehran, Antonio Colombo, Eric Boerwinkle, Christie Ballantyne, William Insull, Robert S Schwartz, Robert Vogel, Patrick W Serruys, Goran K Hansson, David P Faxon, Sanjay Kaul, Helmut Drexler, Philip Greenland, James E Muller, Renu Virmani, Paul M Ridker, Douglas P Zipes, Prediman K Shah, and James T Willerson. From vulnerable plaque to vulnerable patient: a call for new definitions and risk assessment strategies: Part I. *Circulation*, 108(14):1664–72, October 2003.
- [6] Roderic Lakes. *Viscoelastic Materials*. Cambridge University Press, 1 edition, 2009.
- [7] M.N.M. Allam and a.M. Zenkour. Bending response of a fiber-reinforced viscoelastic arched bridge model. *Applied Mathematical Modelling*, 27(3):233–248, March 2003.
- [8] R. Lewandowski and B. Choryczewski. Identification of the parameters of the Kelvin-Voigt and the Maxwell fractional models, used to modeling of viscoelastic dampers. *Computers & Structures*, 88(1-2):1–17, January 2010.
- [9] Damian Craiem and Ricardo L Armentano. A fractional derivative model to describe arterial viscoelasticity. *Biorheology*, 44(4):251–263, January 2007.
- [10] Damian Craiem, Francisco J Rojo, José Miguel Atienza, Ricardo L Armentano, and Gustavo V Guinea. Fractional-order viscoelasticity applied to describe uniaxial

- stress relaxation of human arteries. *Physics in medicine and biology*, 53(17):4543–54, September 2008.
- [11] Jia Guo Liu and Ming Yu Xu. Higher-order fractional constitutive equations of viscoelastic materials involving three different parameters and their relaxation and creep functions. *Mechanics of Time-Dependent Materials*, 10(4):263–279, March 2006.
- [12] R. L. Bagley and P. J. Torvik. On the Fractional Calculus Model of Viscoelastic Behavior. *Journal of Rheology*, 30(1):133, 1986.
- [13] Igor Podlubny. *Fractional Differential Equations*. Academic Press, 1 edition, 1999.
- [14] Severino P. C. Marques and Guillermo J. Creus. *Computational viscoelasticity*. Springer Heidelberg, 2012.
- [15] Ricardo L. Armentano, J.G. Barra, and J. Levenson. Arterial Wall Mechanics in Conscious Dogs Assessment of Viscous, Inertial, and Elastic Moduli to Characterize Aortic Wall Behavior. *Circulation Research*, 76(3):468–478, 1995.